Available online at http://scik.org
Commun. Math. Biol. Neurosci. 2024, 2024:88
https://doi.org/10.28919/cmbn/8686
ISSN: 2052-2541

THE PERFORMANCE OF LONG MEMORY FRACTIONAL SERIES PRICE MODEL OF ESSENTIAL TRACE ELEMENT ZINC

ERMAN ARIF[1], ELIN HERLINAWATI[2], DODI DEVIANTO[3,*], MUTIA YOLLANDA[3], AFRIMAYANI AFRIMAYANI[4]

[1]Information System Study Program, Universitas Terbuka, Tangerang Selatan 15418, Indonesia
[2]Mathematics study program, Universitas Terbuka, Tangerang Selatan 15418, Indonesia
[3]Department of Mathematics and Data Science, Universitas Andalas, Padang 25163, Indonesia
[4]Mathematics Study Program, UIN Imam Bonjol Padang, Padang 25171, Indonesia

Abstract. Zinc is an essential trace element metal commodity that plays an important role in the economy because it is used as a raw material in various industries such as medicine, biological process, electronic devices, building construction, cement, and textiles. This study aims to build the pattern of zinc futures price movement in the form of linear and nonlinear model. An autoregressive fractionally integrated moving average (ARFIMA) and Double Exponential Smoothing (DES) as linear models were developed for time series data containing the exponential and long memory effects where the order can be formed fractionally, respectively. In contrast, Long Short-Term Memory as nonlinear model demonstrating the neurons system function also utilized to build the model of zinc price. In determining the prefered model of zinc price, three models of ARFIMA, DES, and LSTM are then compared by using MAE, RMSE, and MAPE, while AIC and BIC are used to measure the best selection model in ARFIMA model. Zinc futures price data shows the ARFIMA and LSTM models with a long memory effect with a high accuracy value, which are better than the classical model of DES. The result shows that zinc futures price has an important role in the industry because the price tends to be stable with a long memory effect as an industrial raw material.

*Corresponding author
E-mail address: ddevianto@sci.unand.ac.id
Received June 09, 2024

Keywords: zinc future price; long memory; ARFIMA; DES; LSTM.

2020 AMS Subject Classification: 62M10, 62M45, 62P10.

1. INTRODUCTION

Zinc is an essential trace element metal commodity that plays an essential role in the economy. Zinc is widely used as a raw material in various industries such as medicine, biological process, electronic devices, building construction, cement, and textiles [1, 2, 3, 4, 5]. According to the London Metal Exchange, every metal needs to fulfill strict quality, lot size, and shape specifications. Zinc contracts demand physical asset delivery for settlement, and the contract's deliverable assets are 25 tons of high-grade zinc. This extensive use of zinc has an impact on its demand that gets higher in each country, rising to the fluctuations in the price of zinc and the industrial production goods using zinc as their raw materials. Even the fluctuations of zinc are affected the industrial processes and economies in a country on a large scale. Therefore, the risk of the fluctuation of zinc price should be minimized by analyzing its pattern data so that a statistical method is required. The movement of zinc price ordered by time can be built into its statistical method using the time series model. Time series data tends to have a recurring pattern, where past periods will repeat themselves in the present or future. Time series model analysis aims to find a short-term or long-term pattern to be applied to decision-making based on forecasting in the next period [6].

The time series data with a short-memory pattern has a unique characteristic: there is a weak correlation of the data in the short period. The most popular model is the Autoregressive Integrated Moving Average (ARIMA). In the ARIMA model, the stationary data in the mean applies the differencing using the non-negative integer number of d [7]. This ARIMA model can be applied using the data on inflation, stocks, and commodity prices [8]. This is because the data tends to be observed based on the order of time to obtain predictions of future data so that policymakers can know the actions that need to be taken for interested parties in the field. In this particular case, the characteristic of the long-memory pattern is a strong correlation in the period. Using the autocorrelation function (ACF), the long-memory pattern that decays slowly over time can be detected. Besides, the stationary data in the mean applies the differencing using the fractional or the non-negative real number of d between 0 and 0.5. This advanced ARIMA

model with fractional integration order d and containing the long-memory effect is well known as Autoregressive Fractional Integrated Moving Average (ARFIMA) model. The stationary process of the ARFIMA model in the mean may estimate its fractional integration order d by using the Geweke and Porter Hudak (GPH) method [9]. The GPH method is used because it can estimate parameters d directly without having to know the value of the autoregressive order (p) and the order of the moving average (q) first [10]. Since the residual assumptions in ARFIMA model has to be fulfilled, this condition sometimes obstructs the researcher to process the data easily and has to pay the attention about the pattern of the data whether the pattern can be classified to be the time series. Fortunately, residual assumptions can be avoided by using a nonlinear model that employs iteration or numerical processing. There are numerous nonlinear techniques that can be categorized as nonlinear models. In this study, recurrent long short-term memory is chosen because its parameters can be adjusted to acquire the optimal weights for each unit. In econometrics, there is also the Vector Autoreggressive that is utilized in economics issue to determine whether one variable to other variable has the impact in each other [11, 12]. This method is usually applied if the number of time series data greater than or equal to two series data.

Research on metal commodity prices has been conducted in [13, 14], finding that zinc has different price movements than most other metal commodities. Further research has compared ARIMA and ARFIMA models to forecast gold prices in Malaysia using MAE, RMSE, and MAPE [15]. The MAE, RMSE, and MAPE results indicate that the ARFIMA model performs better in forecasting gold prices than the ARIMA model. In an advanced case, the ARFIMA model can be combined with the Poisson distribution by ascertaining non-negative credibility per period in the affine prediction of frequency risks [16]. Therefore, in this study the zinc price model is then applied ARFIMA model than ARIMA model. Beside, the previous research about nonlinear model, especially neural networks as the machine learning methods, are already published. According to the backpropagation methods as the part of neural networks methods, the parameters of weights are adjusted by using numerical processing so that the optimal weights are obtained [17, 18].

In the environment of the nervous system study, the neuroscience is widely used in demonstrating how the human brain working to process the information and interpretating the results to the problem. Neural networks is one of the neurosciece that is applied the nervous system using some iteration to have the optimal weights that is associated to their input unit. Long Short-Term Memory (LSTM) model, belonging to the category of recurrent neural network, effectively overcomes the challenge of vanishing gradients that often arise in training. Its versatility allows for application across various topics, including the intricate and volatile financial market [19], and specific cases such as asset pricing in the Chinese stock market [20], due to its ability to mitigate error propagation during iterations. Neural network also finds usefulness in predicting energy demand and CO_2 emissions [21]. In this study, a fusion of a multiobjective mathematical model with data-driven machine learning algorithms enhances the accuracy of energy demand and CO_2 emissions forecasts in the transportation sector.

The development of the ARFIMA model on various commodity prices provides essential information about the effects of long-memory data. The change in zinc price is detected as having a long-memory pattern based on the autocorrelation function that decays slowly and forms the cosine function. Beside, this pattern is also proceed by using the machine learning method of long-short term memory (LSTM) model. Therefore, this study will analyze the zinc price model using the ARFIMA, DES, and Recurrent LSTM models to detect the effect of long memory on zinc price movements. Then, the preferred model will be chosen by using the measurement accuracy of Mean Absolute Error (MAE), Root Mean Square Error (RMSE), and Mean Absolute Percentage Error (MAPE).

2. Material and Methods

2.1. Data Source. In this study, the secondary data of zinc price with a monthly period is accessed on the investing website, www.investing.com, which started from October 2015 to April 2024.

2.2. The Building of Classical Autoregressive Fractional Integrated Moving Average Model. A random variable series $\{X_t\}$ is characterized as a sequence of white noise while an independent random variable with a specified distribution maintains a constant mean of zero

and a constant variance of $Var(X_t) = \sigma^2$ for $k \neq 0$. ARIMA, a classical time series model, combines AR and MA models after integer differencing. ARIMA evolved into ARFIMA, which incorporated ARFIMA features. ARFIMA has the same structure as ARIMA but uses fractional values for differencing rather than integer differencing. Let $\phi_p(B)$ as AR components, $\theta_q(B)$ as MA components, B as the operator of backward shift, and $(1-B)^d X_t$ indicates the d-order differenced stationary time series with $0 < d < 0.5$, the process is labeled ARFIMA(p, d, q) [22]:

$$\phi_p(B)(1-B)^d X_t = \theta_q(B)\varepsilon_t \tag{1}$$

with

$$\begin{aligned} \phi_p(B) &= (1 - \phi_1 B - \phi_2 B^2 - \cdots - \phi_p B^p) \\ \theta_q(B) &= (1 - \theta_1 B - \theta_2 B^2 - \cdots - \theta_q B^q) \end{aligned}$$

where p, q, and B are the positive integer values. The ARFIMA model is built in the following phases.

(1) Examining the data's stationarity in terms of variance. Since the data was not stationary, data transformation was used to get a rounded value (λ). Assuming that the data X_t is non-stationary in terms of variance, it can be transformed employing the formula $T(X_t) = (X_t^{\lambda-1})/\lambda$, where λ is the transformation parameter. Since $\lambda = 1$, a rounded value process is obtained, and stationarity is achieved [10].

(2) Identifying the ARFIMA model. The ARFIMA model is determined its candidate models by combining the order of MA(q) and AR(p) using the significant lag of ACF and PACF, respectively.

(3) Employing the Geweke and Porter-Hudak models, calculate the differentiating parameters using the following formula [10]:

$$\widehat{d}_{GPH} = \frac{\sum_{j=1}^{m}(x_j - \bar{x})(y_j - \bar{y})}{\sum_{j=1}^{m}(x_j - \bar{x})^2} \tag{2}$$

The least maximum square method is used to determine the value of d_{GPH}, which is then examined using the spectral density logarithm equation. The estimated integration

order d is more flexible because it is performed without beforehand knowing the values of the orders p and q.

(4) Transforming the differential data using the obtained $\widehat{d}_{GPH}$ values.

(5) Performing parameter estimation and signification tests of the ARFIMA model.

(6) Identifying potential ARFIMA model by combining significant orders of autoregressive (AR) and moving average (MA) models using PACF and ACF plots of stationary data, respectively.

(7) Estimating parameters and testing the significance of ARFIMA model. Parameter estimation is performed on each model, followed by significance tests. A model is considered feasible when its parameters are significant, with probability values smaller than $\alpha = 5\%$.

(8) Choosing the optimal ARFIMA model based on the least Akaike Information Criterion (AIC) and Bayesian Information Criterion (BIC).

When fitting ARFIMA model, potentially significant models were selected, and the best model was selected. The goodness-of-fit criteria such as AIC, BIC, and HQ were applied, using the loglikelihood function to determine the best model. Let $\hat{\sigma}_{\varepsilon}^2$ represent the maximum likelihood estimator of σ_{ε}^2, k denoted the number of estimated parameters, and n indicated the number of observations. The equations for AIC, BIC, and HQ were systematically written as follows:

$$AIC = n\, ln(\hat{\sigma}_{\varepsilon}{}^2) + 2k \tag{3}$$

$$BIC = n\, ln(\hat{\sigma}_{\varepsilon}{}^2) + k ln(n) \tag{4}$$

$$HQ = n\, ln(\hat{\sigma}_{\varepsilon}{}^2) + 2k ln(ln(n)) \tag{5}$$

The best model was selected based on the smallest value among AIC, BIC, and HQ. Assuming there were two smallest values in any of these criteria, a nonparametric model was required to determine the smallest rank.

(9) Testing the residual assumptions of the best ARFIMA model, including non-autocorrelation and normality.

The fitted ARFIMA model was then extended into a time series analysis to assess whether the residual assumptions were met. It is important to point out that these assumptions started with autocorrelation and progressed to heteroscedasticity and normality. The initial hypothesis suggested that there was no linear dependency connection in the residual ARFIMA model. The statistic value could be expressed as follows [22]:

$$Q_{LB} = n(n+2)\sum_{i=1}^{k}\frac{\rho_i^2}{n-i} \tag{6}$$

where n is the number of data, the sample auto-correlation coefficient at lag $k = 1,2,3,\cdots,K$ is denoted as ρ_i^2, and lag length is denoted as K. The initial hypothesis was rejected when the statistic value was greater than the critical value or $Q_{LB} > \chi_\alpha^2(k-p-q)$. On the other hand, the hypothesis could be rejected assuming the probability value was less than the significance level.

The second assumption concerned the heteroscedasticity effect using the Lagrange Multiplier (LM) test by White. The initial hypothesis of the LM test assumed that the residual ARFIMA model exhibited homoscedasticity, where the variance of this residual model remained constant, allowing the random fluctuated data to be ignored. The statistic value of the LM test was the product of the determination coefficient value R^2 and the sample size n, expressed as follows:

$$LM = nR^2 \tag{7}$$

The LM test followed a chi-squared distribution with degrees of freedom equal to $k-1$, where k was the number of estimated parameters. The initial hypothesis was rejected because the statistic value was greater than the critical value $LM > \chi_\alpha^2(k-1)$. However, the hypothesis could be rejected when the probability value was less than the significance level.

The final assumption was the normality test, where the initial hypothesis stated that the residual skewness (S) and kurtosis (K) of ARFIMA model matched a normal distribution with expected values of zero. This was determined using the Jarque-Bera (JB) test, and the statistics test of JB could be expressed as follows [22]:

(8) $$JB = \frac{n}{6}\left(S^2 + \frac{(K-3)^2}{4}\right)$$

where K and S are kurtosis and skewness, respectively. The initial hypothesis was rejected since the statistic value was greater than the critical value $JB > \chi^2_\alpha(2)$ or when the probability value was less than the significance level of 5%.

(10) Determining the best ARFIMA model equation and its interpretation.

2.3. The Building of The Double Exponential Smoothing. There are several techniques in time series analysis that, while rudimentary, have retained their implicational value, notably in the domains of forecasting and filtering, due to their simplicity and precision. A time series dataset is forecasted using exponential smoothing. This strategy entails constant improvement based on the most recent observations available. Several generic approaches are utilized in this area, including the single Exponential Smoothing method [23], which is used as an effective time series technique for time series data following a stationary model with trend term. The principles used in this study are derived.

Since most time series data is not stationary, SES is not a useful tool for most applications. To address this issue, Charles Holt has modified the SES to Holt's Exponential Smoothing or Double Exponential Smoothing (DES) or Second-Order Exponential Smoothing which can handle these linear trends. Double Exponential Smoothing is the specified smoothing method which handles time series data with trend. Holt smooths trend values with parameters that are different from the parameters used in the original data smoothing. Holt method has two-parameter double exponential smoothing, that are α and γ that are selected by the smallest value of mean squared error. The double exponential smoothing (DES) can be calculated as follows [24]:

(9) $$\text{Smoothing} \quad : \quad S_t = \alpha X_t + (1-\alpha)(S_{t-1} + r_{t-1})$$

(10) $$\text{Smoothing of trend} \quad : \quad r_t = \gamma(S_t + S_{t-1}) + (1-\gamma) r_{t-1}$$

(11) $$\text{Forecasting} \quad : \quad F_{t+m} = S_t + r_t(m)$$

(12) $$\text{Initialization} \quad : \quad S_1 = X_1$$

$$r_1 = X_2 - X_1 \tag{13}$$

where X_t is actual value or time series data in period t, S_t is single exponential smoothing value in period t, S_{t-1} is single exponential smoothing value in period $(t-1)$, α is the parameter of exponential smoothing for $0 < \alpha < 1$, r_t is trend adjustment increment in period t, r_{t-1} is trend adjustment increment in period $(t-1)$, γ is the parameter of exponential smoothing with trend for $0 < \gamma < 1$, m is the number of periods for forecasting value, and F_{t+m} is forecasted value in period $(t+m)$.

The main characteristic of exponential smoothing is that it smooths the original sequence before using the smoothed sequence to estimate future price values of the variable. This procedure is most useful when the parameters linked to the time series change gradually over time. The exponential smoothing prediction method estimates future values by taking a weighted average of previous observations. This method is useful for forecasting series revealing trends, seasonality, or both.

2.4. The Building of Recurrent Long Short Term Memory Model. In building model of time series, nonlinear model is an alternative method that can ignore to fulfill the residual assumption. Therefore, it will make it easier to build the time series model. Nonlinear model is widely used than linear model because the most real data can be impacted by many factors and it can be make big difference when the indicator is changed. In order to recognize the pattern of data, nonlinear model is required. Neuroscience is one of study that is demonstrating the neurons system function. It means that the information that is received is then continued to be processed until the results is obtained. Neural networks is one of nonlinear model that is applied for many problems. Because the neuron in neural networks has the relationship between on input unit into its weight, it makes the process need the iteration and validtation to make sure the obtained networks has a good performance [17]. In this study, one of the neural networks, that is long short-term memory (LSTM) is applied. LSTM model can overcome the outlier data with the iteration processing so that the error of the model getting smaller. The persistent vanishing/exploding gradient problem resulting from long-term dependencies, even with substantial data, posed a challenge due to the random fluctuation in residuals. Consequently, the application of LSTM neural network was deemed necessary [25].

In the framework of big data analysis, it was conceivable to foretell the future by recognizing patterns in historical data. Furthermore, there was a link between the variables and the historical data or data residuals. The artificial neural network was a device that simulated the network of nerve cells seen in human and animal brains [17]. It also had a few hidden layers that connected the input layer to the output layer. Weights and biases, often known as network coefficients, specified the connections between two layers. Figure 1 represented the general construction of the mathematical neural network model [22].

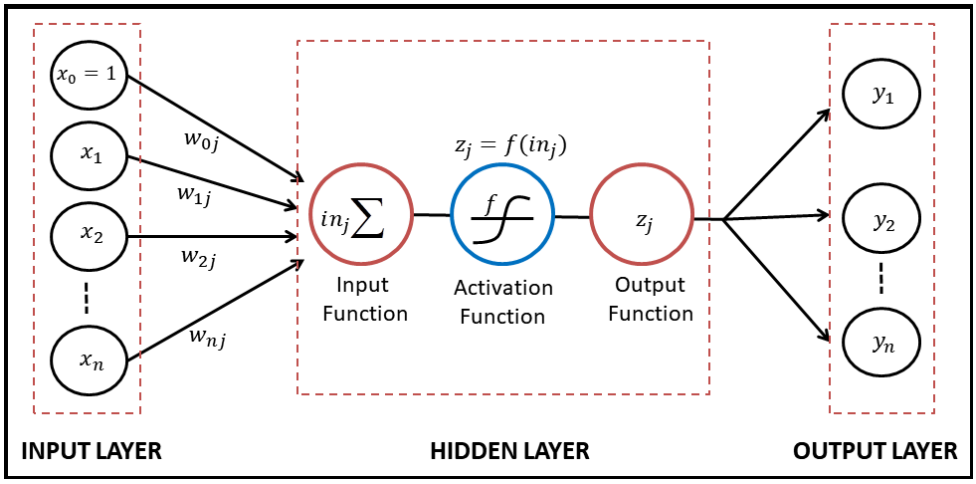

FIGURE 1. A diagram construction of mathematical neural network model

Figure 1 showed the construction of neural network that connected two layers through directed links of weights or biases to determine the sign and strength of the input data. The input data x_i, representing $x_1, x_2, \cdots, x_n$ was then calculated as a weighted sum of its inputs on the hidden layer, in_j. Each hidden unit j transformed the input through the activation function f, yielding z_j, expressed as follows:

$$z_j = f(in_j) = f\left(\sum_{i=0}^{n} x_i w_{ij}\right) \tag{14}$$

This result was then passed as input to other neurons and the activation function f scaled the output z_j into appropriate ranges. The network architecture could be classified as feed-forward (FFNN) and recurrent neural network (RNN), commonly used for forecasting. In a feed-forward network, each input unit received data from the layer below. Meanwhile, the outputs of a recurrent network became inputs in the preceding layer. The recurrent network created a dynamical

system where inputs depended on the initial values of previous inputs, in order to simulate a stable state [22]. A common type of recurrent neural network was LSTM, designed for analyzing time series data. LSTM was equipped to handle long-term dependencies present in time series data, ensuring outcomes depended on previous data values.

In constructing the structural LSTM model, LSTM neural network comprised input gates, memory cells, forget gates, and output gates. These components processed information over longer periods. The network could selectively store and retrieve information as needed, regulated by these gates that controlled the flow of data into and out of memory cells. The input gate introduced new inputs to the cell, the forget gate maintained values for later use, and the output gate determined the output of the cell. Common tasks for which LSTM were employed included language translation, speech recognition, and stock price prediction. While RNN could learn long-term dependencies in data, it was impacted by the vanishing gradient problem. LSTM addressed this issue by using a set of gates to determine the data to retain and those to discard. This allowed the model to retain more information compared to RNN, achieved through gradient control [26]. A typical LSTM cell structure could be seen in Figure 2.

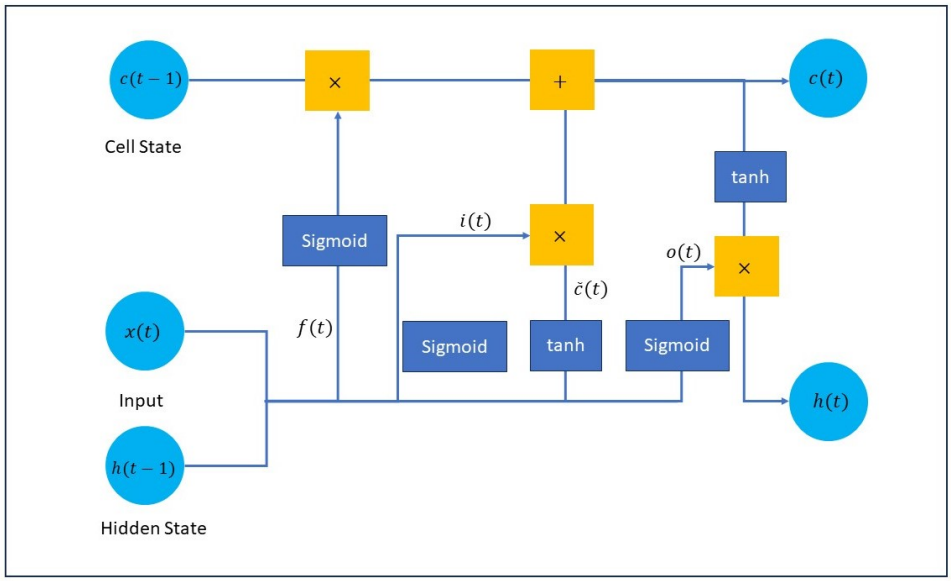

FIGURE 2. A diagram construction of mathematical long short-term memory neural network model.

The mathematical expressions for the inner connections of the gates in LSTM cell structure were as follows. Let $f(t), i(t), c(t)$, and $o(t)$ as forget gate, input gate, modulation cell gate, and output gate respectively with their activation functions of sigmoid, sigmoid, tanh, and sigmoid, respectively. In the modulation cell gate, the input is updated at the present time instant. All gates work on current input $x(t)$ and previous values of states $h(t-1)$. The design of deep network generally involved multiple hidden layers. To achieve the best results in the proposed work, several LSTM hidden layer topologies were evaluated.

In validation model, the testing process of LSTM model has to have smaller value of model evaluation than training process. It means that the LSTM model can recognize the new data and can be used to forecast the next value in the next period.

2.5. Model Evaluation. In modeling, evaluation criteria were used to assess how well it predicted output values from input data [27]. The Mean Squared Error (MSE) measured the gap between actual values and projected values. It was calculated by averaging squared differences between expected and actual numbers. A lower MSE value indicated a more accurate model.

$$MSE = \frac{SSE}{n} = \frac{\sum_{t=1}^{n}(y_t - \hat{y}_t)^2}{n} \tag{15}$$

The accuracy of a model was quantified by the Mean Absolute Percentage Error (MAPE), expressed as a percentage. It was computed by dividing the absolute difference between expected and actual values by the actual value, then averaging these percentages and calculating the difference between predicted and actual values. A lower MAPE number indicated better real-world prediction by the model.

$$MAPE = \frac{1}{n}\sum_{t=1}^{N}\frac{|y_t - \hat{y}_t|}{y_t} \times 100\% \tag{16}$$

Another model to measure the gap between expected and actual values was the Mean Absolute Error (MAE). This was calculated by finding the absolute difference between expected and actual numbers, and then taking their average. The MAE statistic also assessed the model accuracy, with lower MAE values indicating higher results.

$$MAE = \frac{1}{n}\sum_{t=1}^{N}|y_t - \hat{y}_t| \tag{17}$$

After calculating the optimal model, the ratio of sums of squares of regression to sums of total squares determined the coefficient R^2. This measurement ranged from 0 to 1, and the value of R^2 close to 0 indicated the estimated model did not fit well, while a value close to 1, implied it was well-fit. Let y be the mean of the dataset y_i, where $i = 1, 2, \cdots, n$. R^2 was calculated as follows:

$$R^2 = \frac{\sum_{i=1}^{n}(\hat{y}_i - \bar{y})^2}{\sum_{i=1}^{n}(y_i - \bar{y})^2} \tag{18}$$

The value of R^2 represented the amount of variance in the response variable explained by the predictor variable. Furthermore, it represented the squared correlation between observed values y_i and anticipated values $\hat{y}_i$ based on data processing.

3. Main Results

This section involved building a long-memory pattern of ARFIMA model, enhancing a long short-term memory model, and evaluating the preferred model using certain criteria.

3.1. Building long-memory pattern of ARFIMA model. In this subsection, the modeling process was identified by the imported dataset, firstly, the dataset can illustrate as graphically using a monthly period of zinc price, which started on October 2015 until June 2023 in the following Figure 3. Figure 3 shows the actual zinc price data started from October 2015 until

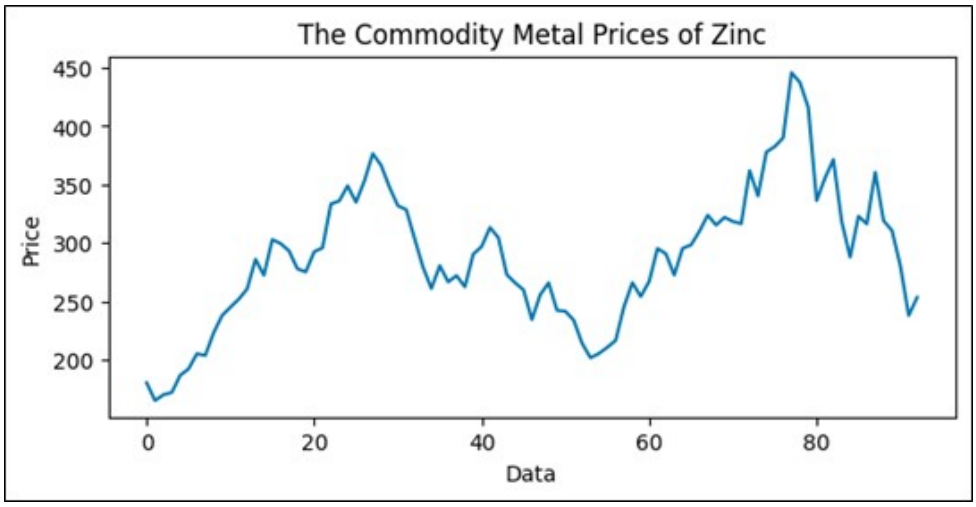

FIGURE 3. The commodity zinc price from October 2015 until June 2023.

June 2023 with monthly period exhibited free fluctuations. Based on Figure 3, the data did not

fluctuate around a constant mean and variance, the data were not stationary concerning mean and variance values. To address this non-stationarity in time series data regarding variance, data transformation was performed using the Box-Cox transformation. The first step was determining the rounded value (λ). Based on the transformation parameter formula, the value of λ was 0.7124, indicating non-stationarity with respect to variance. Therefore, a second-stage transformation was conducted with a λ value of 1, rendering the inflation data stationary regarding variance. The subsequent step was to check whether the data were stationary concerning mean values using the Augmented Dickey-Fuller test, shown in Table 1.

TABLE 1. Augmented Dickey-Fuller Test.

Critical Value	**ADF Test**	
	Statistics Value	**p-value**
1% : −3.5035		
5% : −2.8935	−2.2648	0.1836
10% : −2.5838		
Observations Used: 92		
Lag Order: 2		

From Table 1, the value of the statistic exceeded the critical value at the 5% significance level, implying that the data were not stationary concerning the mean value. This was further supported by the probability value of 0.1836, which was higher than the 5% significance level. To determine the order differencing of fractional or integer, the identification pattern used the Autocorrelation Function (ACF) to ascertain the presence of long-memory terms as shown in Figure 4.

Figure 4 showed a gradual decrease in data over time, indicating the presence of a long-memory pattern and suggesting a fractional order differencing for the model. Mathematically, differencing with an order value of d was required to make the data stationary concerning the mean, estimated using the Geweke Porter-Hudak (GPH) model. The order model determined by the GPH model was $\hat{d}_{GPH} = 0.4662$. As $\hat{d}_{GPH} = 0.4662$ was less than 0.05, the data exhibited a long-memory effect and could be modeled with ARFIMA. Subsequently, the order of ARFIMA

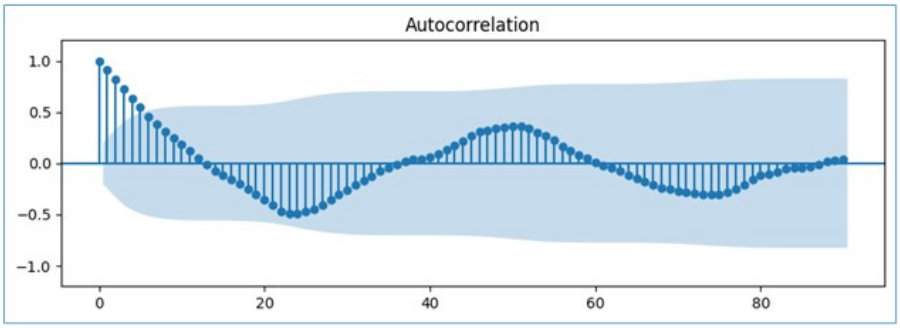

FIGURE 4. ACF plot of zinc data exhibiting variance and mean stationarity

model was determined by identifying the number of significant lags in the ACF and PACF plots, as shown in Figure 5.

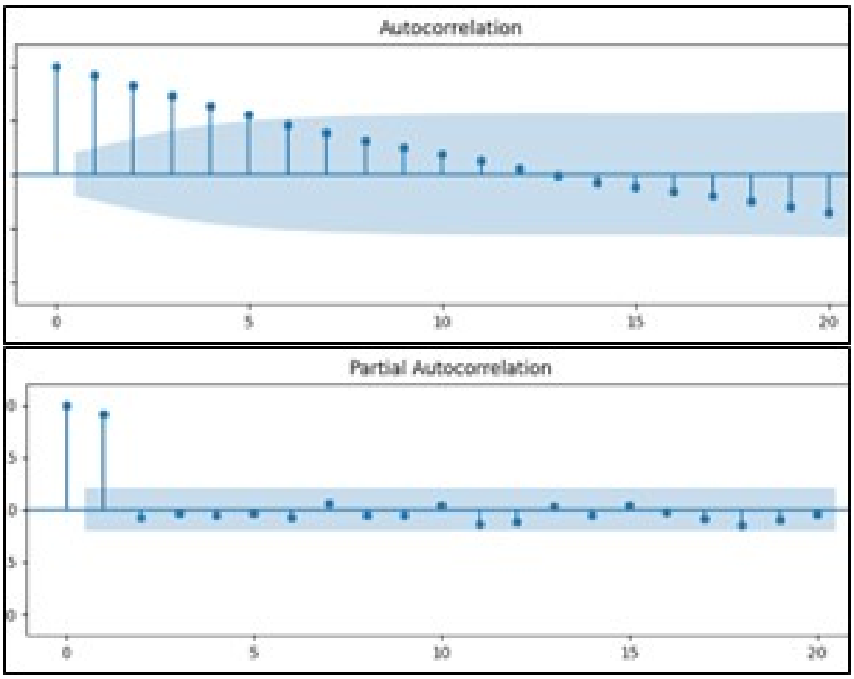

FIGURE 5. Plot of autocorrelation and partial autocorrelation function

Based on Figure 5, the ACF coefficient reached a significant value at a lag of 6, while the PACF coefficient reached a significant value at a lag of 2. This suggested the possibility of forming an ARFIMA model by combining a maximum lag of 2 for parameter p and a maximum lag of 6 for parameter q, along with a d_{GPH} value of 0.4662. Furthermore, the parameters for each model were estimated and from the results, a significance test was conducted. The

probability values for each model were shown in Table 2. A model was considered significant when the probability value of its parameter was less than 0.05.

TABLE 2. The significant estimated parameters of the ARFIMA model.

Model	**Estimated Parameter**				**Model selection**	
	Parameter	**Estimate**	**Statistic**	**Pr($>\|z\|$)**	**AIC**	**BIC**
ARFIMA(0, 0.4662,1)	(MA(1))	-0.4744	-6.1857	6.18E-10	604.5811	614.7115
ARFIMA(0, 0.4662,2)	(MA(1))	-0.5195	-5.3523	8.69E-08	596.0423	608.7053
	(MA(2))	-0.332	-3.5071	4.53E-04		
ARFIMA(0, 0.4662,3)	(MA(1))	-0.5264	-4.9611	7.01E-07	594.3939	609.5895
	(MA(2))	-0.3379	-3.4335	5.96E-04		
	(MA(3))	-0.2039	-2.0238	4.30E-02		
ARFIMA(0, 0.4662,5)	(MA(1))	-0.5119	-4.9723	6.62E-07	586.9969	607.2577
	(MA(2))	-0.3994	-3.8723	1.08E-04		
	(MA(3))	-0.3505	-3.3699	7.52E-04		
	(MA(4))	-0.3999	-3.6922	2.22E-04		
	(MA(5))	-0.3775	-3.3496	8.09E-04		
ARFIMA(1, 0.4662,0)	(AR(1))	0.6249	7.9502	1.86E-15	587.4473	597.5777
ARFIMA(1, 0.4662,1)	(AR(1))	0.8142	9.0539	1.38E-19	585.7271	598.3901
	(MA(1))	0.3262	2.1706	3.00E-02		
ARFIMA(1, 0.4662,3)	(AR(1))	-0.8301	-7.089	1.35E-12	597.0106	614.7388
	(MA(1))	-1.398	-9.281	1.68E-20		
	(MA(2))	-0.7968	-4.8999	9.58E-07		
	(MA(3))	-0.3531	-4.1859	2.84E-05		
ARFIMA(2, 0.4662,0)	(AR(1))	0.5069	5.0139	5.33E-07	586.2801	598.9431
	(AR(2))	0.1877	1.7999	7.19E-02		

Table 2 shows that the ARFIMA models that is obtained: ARFIMA$(0, 0.4662, 1)$, ARFIMA$(0, 0.4662, 2)$, ARFIMA$(0, 0.4662, 3)$, ARFIMA$(0, 0.4662, 4)$,

ARFIMA$(1,0.4662,0)$, ARFIMA$(1,0.4662,1)$, and ARFIMA$(1,0.4662,3)$ were significant and suitable for building an ARFIMA model. However, not all significant models were applied in the subsequent steps. In order to identify the optimal model, a comparison was made between the AIC and BIC values. The evaluation of these values in Table 2 for the seven models revealed that the ARFIMA$(1,0.4662,1)$ showed the lowest AIC and BIC values among the available alternatives. Consequently, it can be stated that the ARFIMA$(1,0.4662,1)$ appeared as the most favorable choice.

Relying solely on model selection was insufficient to confirm that ARFIMA$(1,0.4662,1)$ adequately fulfilled the necessary conditions as a time series. This led to the examination of the residual assumption of the ARFIMA$(1,0.4662,1)$. Table 3 showed a test of residual assumptions for ARFIMA$(1,0.4662,1)$.

TABLE 3. Residual assumption test of ARFIMA $(1,0.4662,1)$ model

Residual Assumption	**Statistic χ^2**	**p-value**
Homoscedasticity	4.5972	0.1004
Autocorrelation	$[0.0004; 70.5490]$	> 0.05
Normality	6.4230	0.0403

Upon reviewing Table 3, it became evident that the p-value of the autocorrelation test had surpassed 0.05 at the 91st lag, indicating the absence of correlation among residuals. However, in the heteroscedasticity and normality tests, the p-values were below 0.05. This suggested the presence of heteroscedasticity or volatility effects on the residuals, necessitating their adjustment. The normality test could be overlooked due to the rapid fluctuations in the time series data. Therefore, ARFIMA$(1,0.4662,1)$ was established as the best model with the following equation:

$$\begin{aligned}(1-B)^d X_t &= \Phi_1 X_{t-1} + \theta_1 \varepsilon_{t-1} + \varepsilon_t \\ (1-B)^{0.4662} X_t &= 0.8142 X_{t-1} + 0.3262 \varepsilon_{t-1} + \varepsilon_t\end{aligned}$$

The following Table 4 shows the forecaste data in the next months.

TABLE 4. Forecasting zinc price data in one months ahead.

Date	Actual Price	Estimated ARFIMA	Lower	Upper	Decision
May, 2024	322.58	307.0051	285.0336	328.9766	in interval

Table 4 presents the actual data, the estimated data using ARFIMA model, and the estimated confidence interval of 95%. Based on Table 4, each actual value is included in the confidence interval of 95%. It shows that the ARFIMA(1, 0.4662,1) model has the best performance to forecast the data in the future so that it can be utilized to minimize the risk for some economic agents or investors.

3.2. Building Double Exponential Smoothing. As the basic technique, the exponential smoothing is utilized to estimate the actual value and then make the forecasting to determine the value in the next period. Classical econometric methods were used to predict the development of zinc price in this study. Considering that the trading activities of the zinc price is still spreading across the world, the focus of this study is to build the model of the double exponential smoothing (DES).

The optimal constant smoothing for this study is $\alpha = 0.9627$ and $\gamma = 0.1153$, so that the DES model can be expressed as

$$\begin{aligned}
\text{Smoothing} &: S_t = \alpha X_t + (1-\alpha)(S_{t-1} + r_{t-1}) = 0.9627X_t + 0.0373(S_{t-1} + r_{t-1}),\\
\text{Smoothing of trend} &: r_t = \gamma(S_t + S_{t-1}) + (1-\gamma)r_{t-1} = 0.1153(S_t + S_{t-1}) + 0.8847r_{t-1},\\
\text{Forecasting} &: F_{t+m} = S_t + r_t(m),\\
\text{Initialization} &: S_1 = X_1 = 180.36,\\
&\quad r_1 = X_2 - X_1 = 165.08 - 180.36 = -15.28.
\end{aligned}$$

Based on the model of double exponantial smoothing (DES), the DES model can be used to forecast the new data in the next period. The following Table 5 shows the forecaste data in the next month, May 2024.

Table 5 presents the actual data, the estimated data using DES model, and the estimated confidence interval of 95%. Based on Table 5, each actual value is included in the confidence

TABLE 5. Forecasting zinc price data in eight months ahead.

Date	Actual Price	Estimated DES	Lower	Upper	Decision
May, 2024	322.58	304.6349	265.891	343.3788	in interval

interval of 95%. It shows that the DES model has the best performance to forecast the data in the future so that it can be utilized to minimize the risk for some economic agents or investors.

3.3. Building Long Short-Term Memory. In building model of time series, nonlinear model is an alternative method that can ignore to fulfill the residual assumption. Therefore, it will make it easier to build the time series model. Nonlinear model is widely used than linear model because the most real data can be impacted by many factors and it can be make big difference when the indicator is changed. In order to recognize the pattern of data, nonlinear model is required. Long short-term memory (LSTM) as the nonlinear model can overcome the outlier data with the iteration processing so that the error of the model getting smaller. Consequently, the application of LSTM neural network was deemed necessary.

Analysis of Zinc price showed that the data continued to exhibit considerable fluctuations, indicating the persistence of volatility in the data. Based on the autocorrelation function of the data, the significant impact is occured at the sixth lag. This observation implied that the zinc price in each month was dependent on the value of the next six month. Consequently, a preferred model aimed at mitigating the fluctuation effect would involved employing 6 as the number of significant lags. To process the data, LSTM neural network, which was a nonlinear model, would be applied. This model included training the network on 75% of the dataset and testing it on the remaining 25% to evaluate performance. Parameter settings for LSTM model were clearly shown in Table 6.

In validating the process, the networks have good performance if mean squared error of testing is less than training. Table 7 shows how the comparison mean squared error between training process and testing process.

Based on Table 7, the mean squared error (MSE) of testing (0.0264) is less than the training process (0.0334). It means that the networks that is built by using the training data have a good

TABLE 6. Parameter settings for LSTM model.

Parameters	**Values**
Total hidden Layers	4
The number of hidden units	4
Optimization approach	Adam
Total repetition (epochs)	1500
Training data	73
Testing data	22

TABLE 7. Validation data.

Process	**Mean Squared Error**
Training	0.0334
Testing	0.0264

performance because the networks can recognize the new data (testing data). Therefore, the networks can be used for forecasting the new data in the next period.

The following Table 8 shows the forecaste data in the next eight months.

TABLE 8. Forecasting zinc price data in eight months ahead.

Date	**Actual Price**	**Estimated LSTM**	**Lower**	**Upper**	**Decision**
May, 2024	322.58	369.3786	306.9120	431.8451	in interval

Table 8 presents the actual data, the estimated data using LSTM model, and the estimated confidence interval of 95%. Based on Table 8, actual value is included in the confidence interval of 95%. It shows that the LSTM model has good performance to forecast the data in the future so that it can be utilized to minimize the risk for some economic agents or investors.

3.4. Evaluating the Estimated Models. After building the models of zinc price, a comparison of ARFIMA, DES, and LSTM models was conducted to evaluate their performance. Figure

6 graphically showed this comparison, including the actual zinc price data, ARFIMA(1, 0.4662, 1), DES and LSTM model. These four representations were respectively depicted in blue, purple, and green. A model that closely associated with the actual value and accurately tracked its movements would likely be more accurate.

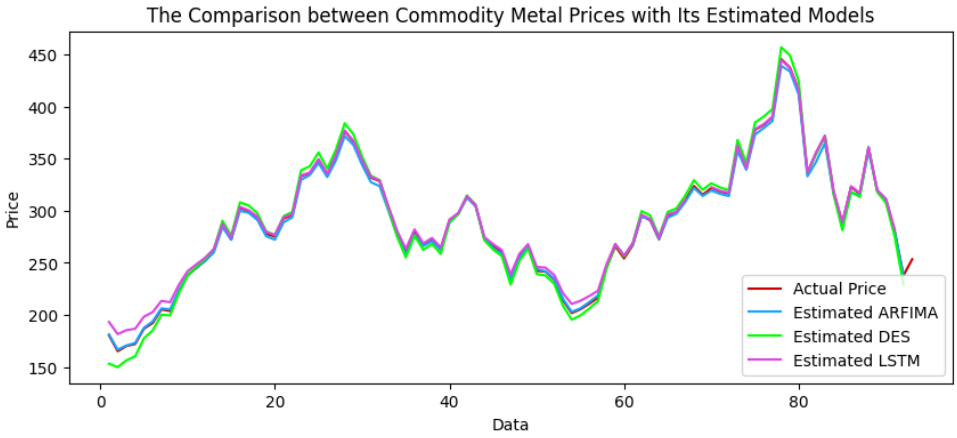

FIGURE 6. Comparison between actual data of inflation and ARFIMA-LSTM model.

The red, blue, purple, and green lines in Figure 6 represented Actual value, ARFIMA, LSTM, and DES models, respectively. These lines smoothly estimated the red line (actual value) using a numerical model to imitate and recognize the actual value. This indicated that the improved models represented by the blue and purple lines closely approximated the red line than green line. Essentially, the blue line can not be compared better than the purple line in estimating the red line because the gap between these both lines are not significantly different, but blue and purple lines are better than the green line because there is agap between green line and the red line In other words, the sensitivity of the fluctuation data, could be effectively handled through the application of numerical models, specifically LSTM neural network and ARFIMA model, but not with DES model. The validity of this statement was supported by evaluating the model using metrics such as MSE, MAE, and MAPE. A comparison between ARFIMA, DES, and LSTM could be seen in Table 9

From Table 9, LSTM model yielded the smallest values for MAE and RMSE, but ARFIMA has the smallest value for MAPE value. Overall, by using the rank method, the LSTM model be

TABLE 9. Evaluation Model.

Model	MAE	RMSE	MAPE
ARFIMA	2.0942	2.6699	0.6840
DES	4.6469	6.0030	1.7876
LSTM	2.0672	2.6455	1.2890

the first rank so that it can be conclude that LSTM has better performance. This outcome suggested that employing the numerical model of LSTM neural network enhanced and refined the predicted zinc price values. After adjusting the long memory pattern of zinc data, the fluctuation of data went through further processing using LSTM to address the vanishing gradient issue inherent in volatility component, often referred to as heteroscedasticity effects. Consequently, the preferred LSTM neural network effectively improved the fluctuation of the data. Mitigating the impact of heteroscedasticity was achieved through either linear or nonlinear models [22]. The application of DES served as a linear model, while using neural network represented the nonlinear. Among the models,neural network of LSTM appeared to be the most effective for addressing the fluctuation when compared to ARFIMA and DES. The results in Table 9 also showed that the neural network employing LSTM outperformed the classical ARFIMA and DES in terms of nonlinear modeling. The results also underscored the optimal performance achieved through the fusion of the neural network and ARFIMA, particularly when applied to zinc price data. The assessment was based on metrics including MSE, MAE, and MAPE.

4. CONCLUSION

In conclusion, this paper proposed three models that can be utilized to predict the zinc price. Three models of Autoregressive Fractional Integrated Moving Average (ARFIMA), Recurrent Long Short-Term Memory (LSTM), and Double Exponential Smoothing (DES) are then proceed to estimate the pattern of the zinc price data. To achieve stability, LSTM neural network established a dynamic system in which the input depended on the initial values of previous inputs based on the neuroscience working. This adaptation brought the network closer to mimicking brain functions while simultaneously increasing its complexity in learning from data.

Recognizing the limitations of the classical long-memory ARFIMA in accurately predicting inflation, this study underscored the necessity for a nonlinear model. This nonlinear strived to approximate the gradient of ARFIMA through numerical computations until a defined threshold error was met. As the basic method of Double Exponential Smoothing (DES) can be utilized to estimate the pattern of the data. Despite capturing the long-pattern data inherent in zinc price, the model did not adequately optimize zinc price prediction.

The evaluation between ARFIMA, LSTM, and DES utilize the MAE, RMSE, and MAPE to measure the performance of the models. The results show that the recurrent long short-term memory has the best performance to estimate the pattern data of commodity zinc price beacause the numerical process helps the adjustment of initial parameters to be optimal parameters and handles the vanishing gradient problem in the networks. The performance of LSTM effectively mitigates the fluctuation issue present in ARFIMA and DES models with the learning rate and process data that requires the iteration and the thresold value that has to be fulfilled.

ACKNOWLEDGMENTS

The authors are grateful to Universitas Terbuka Indonesia for their support with contract number B/53/UN31.LPPM/PT.01.03/2023.

CONFLICT OF INTERESTS

The authors declare that there is no conflict of interests.

REFERENCES

[1] D.A.M. Osman, O. Nur, M.A. Mustafa, Reduction of energy consumption in cement industry using zinc oxide nanoparticles, J. Mater. Civ. Eng. 32 (2020), 04020124. https://doi.org/10.1061/(asce)mt.1943-5533.0003196.

[2] T. Gupta, S.N. Sachdeva, Study of mechanical, micro-structural and environmental properties of concrete containing zinc industry waste for pavements, Constr. Build. Mater. 245 (2020), 118331. https://doi.org/10.1016/j.conbuildmat.2020.118331.

[3] P.J. Usha, H.B. Aravinda, Removal of zinc and iron metal ions from steel industry effluent using rice husk as an adsorbent, Int. Res. J. Eng. Technol. 7 (2020), 2526–2532.

[4] R. Huang, S. Zhang, W. Zhang, X. Yang, RETRACTED: Progress of zinc oxide-based nanocomposites in the textile industry, IET Collab. Intell. Manuf. 3 (2021), 281–289. https://doi.org/10.1049/cim2.12029.

[5] S. Panhwar, J.A. Buledi, D. Mal, et al. Importance and analytical perspective of green synthetic strategies of copper, zinc, and titanium oxide nanoparticles and their applications in pathogens and environmental remediation, Curr. Anal. Chem. 17 (2021), 1169–1181. https://doi.org/10.2174/1573411017999201125124513.

[6] R.S. Tsay, Analysis of financial time series, Wiley, 2005.

[7] W.W.S. Wei, Multivariate time series analysis and applications, Wiley, 2019.

[8] M.L. Rahman, M. Islam, M. Roy, Modeling inflation in Bangladesh, Open J. Stat. 10 (2020), 998–1009. https://doi.org/10.4236/ojs.2020.106056.

[9] M. Monge, J. Infante, A fractional ARIMA (ARFIMA) model in the analysis of historical crude oil prices, Energy Res. Lett. 4 (2023), 1–3. https://doi.org/10.46557/001c.36578.

[10] D. Devianto, K. Ramadani, Maiyastri, et al. The hybrid model of autoregressive integrated moving average and fuzzy time series Markov chain on long-memory data, Front. Appl. Math. Stat. 8 (2022), 1045241. https://doi.org/10.3389/fams.2022.1045241.

[11] M. Yollanda, W. Harjupa, D. Devianto, et al. Prediction of CENS, MJO, and extreme rainfall events in Indonesia using the VECM model, in: A. Basit, E. Yulihastin, S.Y. Cahyarini, et al. (Eds.), Proceedings of the International Conference on Radioscience, Equatorial Atmospheric Science and Environment and Humanosphere Science, Springer Nature Singapore, Singapore, 2023: pp. 367–383. https://doi.org/10.1007/978-981-19-9768-6_35.

[12] F. Nauval, M. Yollanda, D. Devianto, et al. Monthly Rainfall prediction using vector autoregressive models based on ENSO and IOD phenomena in Cilacap, in: A. Basit, E. Yulihastin, S.Y. Cahyarini, et al. (Eds.), Proceedings of the International Conference on Radioscience, Equatorial Atmospheric Science and Environment and Humanosphere Science, Springer Nature Singapore, Singapore, 2023: pp. 395–406. https://doi.org/10.1007/978-981-19-9768-6_37.

[13] A. Ghoshray, M. Pundit, Economic growth in China and its impact on international commodity prices, Int. J. Finance Econ. 26 (2020), 2776–2789. https://doi.org/10.1002/ijfe.1933.

[14] T. Olofsson, Do commodity prices incentivize exploration permit application? An explorative study of an anecdotal relation, Miner. Econ. 35 (2021), 133–141. https://doi.org/10.1007/s13563-021-00277-0.

[15] A.N.A.M. Azan, N.F.A.M.Z. Mototo, P.J.W. Mah, The Comparison between ARIMA and ARFIMA model to forecast kijang emas (gold) prices in Malaysia using MAE, RMSE and MAPE, J. Comput. Res. Innov. 6 (2021), 22–33. https://doi.org/10.24191/jcrinn.v6i3.225.

[16] J. Pinquet, Positivity properties of the ARFIMA $(0,d,0)$ specifications and credibility analysis of frequency risks, Insurance: Math. Econ. 95 (2020), 159–165. https://doi.org/10.1016/j.insmatheco.2020.10.001.

[17] M. Yollanda, D. Devianto, H. Yozza, Nonlinear modeling of IHSG with artificial intelligence, in: 2018 International Conference on Applied Information Technology and Innovation (ICAITI), IEEE, Padang, Indonesia, 2018: pp. 85–90. https://doi.org/10.1109/ICAITI.2018.8686702.

[18] D. Devianto, F. Wulandari, F. Yanuar, et al. An improvement of parameter estimation accuracy of structural equation modeling using hybridization of artificial neural network in the entrepreneurship structural model, Appl. Math. Nonlinear Sci. 8 (2023), 2279–2302. https://doi.org/10.2478/amns.2023.1.00411.

[19] K. Gajamannage, Y. Park, D.I. Jayathilake, Real-time forecasting of time series in financial markets using sequentially trained dual-LSTMs, Expert Syst. Appl. 223 (2023), 119879. https://doi.org/10.1016/j.eswa.2023.119879.

[20] S. Pan, S. Long, Y. Wang, et al. Nonlinear asset pricing in Chinese stock market: A deep learning approach, Int. Rev. Financial Anal. 87 (2023), 102627. https://doi.org/10.1016/j.irfa.2023.102627.

[21] M.E. Javanmard, Y. Tang, Z. Wang, et al. Forecast energy demand, CO2 emissions and energy resource impacts for the transportation sector, Appl. Energy. 338 (2023), 120830. https://doi.org/10.1016/j.apenergy.2023.120830.

[22] D. Devianto, M. Yollanda, M. Maiyastri, et al. The soft computing FFNN method for adjusting heteroscedasticity on the time series model of currency exchange rate, Front. Appl. Math. Stat. 9 (2023), 1045218. https://doi.org/10.3389/fams.2023.1045218.

[23] R.R. Yager, Exponential smoothing with credibility weighted observations, Inf. Sci. 252 (2013), 96–105. https://doi.org/10.1016/j.ins.2013.07.008.

[24] C.C. Holt, Forecasting seasonals and trends by exponentially weighted moving averages, Int. J. Forecast. 20 (2004), 5–10. https://doi.org/10.1016/j.ijforecast.2003.09.015.

[25] A. Shewalkar, D. Nyavanandi, S.A. Ludwig, Performance evaluation of deep neural networks applied to speech recognition: RNN, LSTM and GRU, J. Artif. Intell. Soft Comput. Res. 9 (2019), 235–245. https://doi.org/10.2478/jaiscr-2019-0006.

[26] S.A. Haider, S.R. Naqvi, T. Akram, et al. LSTM neural network based forecasting model for wheat production in Pakistan, Agronomy. 9 (2019), 72. https://doi.org/10.3390/agronomy9020072.

[27] B. Gülmez, Stock price prediction with optimized deep LSTM network with artificial rabbits optimization algorithm, Expert Syst. Appl. 227 (2023), 120346. https://doi.org/10.1016/j.eswa.2023.120346.